

Spin freezing and slow magnetization dynamics in geometrically frustrated magnetic molecules with exchange disorder

This article has been downloaded from IOPscience. Please scroll down to see the full text article.

2010 J. Phys.: Condens. Matter 22 216007

(<http://iopscience.iop.org/0953-8984/22/21/216007>)

View [the table of contents for this issue](#), or go to the [journal homepage](#) for more

Download details:

IP Address: 147.155.96.14

The article was downloaded on 06/05/2010 at 15:53

Please note that [terms and conditions apply](#).

Spin freezing and slow magnetization dynamics in geometrically frustrated magnetic molecules with exchange disorder

C Schröder^{1,2}, X Fang², Y Furukawa², M Luban², R Prozorov²,
F Borsa^{2,3} and K Kumagai⁴

¹ Department of Engineering Sciences and Mathematics, University of Applied Sciences
Bielefeld, D-33602 Bielefeld, Germany

² Ames Laboratory and Department of Physics and Astronomy, Iowa State University, Ames,
IA 50011, USA

³ Dipartimento di Fisica 'Alessandro Volta' e Unità CNISM, Università di Pavia,
I-27100 Pavia, Italy

⁴ Department of Physics, Faculty of Science, Hokkaido University, Sapporo 060-0810, Japan

E-mail: christian.schroeder@fh-bielefeld.de

Received 3 December 2009, in final form 8 April 2010

Published 5 May 2010

Online at stacks.iop.org/JPhysCM/22/216007

Abstract

We show that intramolecular exchange disorder recently found in the geometrically frustrated magnetic molecules $\{\text{Mo}_{72}\text{Fe}_{30}\}$ and $\{\text{Mo}_{72}\text{Cr}_{30}\}$ leads, in a classical Heisenberg model description, to spin freezing and slow magnetization dynamics reminiscent of spin glass behaviour. Also we suggest that our low temperature and low magnetic field nuclear magnetic resonance (NMR) measurements on $\{\text{Mo}_{72}\text{Fe}_{30}\}$, showing rapid and strong broadening of the proton line width on cooling below 600 mK, are evidence for a crossover from paramagnetic behaviour to a frozen spin configuration. Similar broadening is observed in $\{\text{Mo}_{72}\text{Cr}_{30}\}$. This observed effect is consistent with our theory of spin freezing and slow magnetization dynamics in these systems due to exchange disorder.

(Some figures in this article are in colour only in the electronic version)

1. Introduction

Geometrical frustration is the source of a variety of fascinating phenomena that have been observed in magnetic materials [1]. It arises in lattices that are composed of magnetically frustrated building blocks, such as antiferromagnetically coupled spins on triangles or tetrahedra. Experimental studies on two-dimensional Kagome lattice compounds (composed of corner-sharing triangles) and three-dimensional pyrochlores (composed of corner-sharing tetrahedra) show spin freezing at sufficiently low temperatures [2]. The origin of this spin freezing has long been puzzling. Theoretical studies have shown that the observed spin glass behaviour cannot be explained by geometrical frustration alone [3–5]. Instead, it has been found that weak exchange randomness in the

classical Heisenberg antiferromagnet on the pyrochlore lattice is responsible for a spin glass transition at a temperature set by the disorder strength [3]. This result is consistent with the accepted view that spin glass behaviour has two prerequisites, frustration and randomness [6]. The combination of both requirements leads to highly degenerate free-energy landscapes with a distribution of barriers between different metastable states, resulting in broken ergodicity below a characteristic spin freezing temperature T_f .

Here we present theoretical evidence for spin freezing and slow magnetization dynamics in two similar *zero-dimensional* strongly frustrated systems, specifically, the pair of Keplerate magnetic molecules abbreviated as $\{\text{Mo}_{72}\text{Fe}_{30}\}$ and $\{\text{Mo}_{72}\text{Cr}_{30}\}$ [7, 8]. We attribute this behaviour to the occurrence of intramolecular exchange disorder of the 30

interacting magnetic ions that has recently been found in both molecules [10]. We also suggest that spin freezing is the source of an increase in the proton line width on cooling that we have observed in NMR measurements in both compounds.

In the magnetic molecules $\{\text{Mo}_{72}\text{Fe}_{30}\}$ and $\{\text{Mo}_{72}\text{Cr}_{30}\}$ the magnetic ions Fe^{III} (spin $s = 5/2$) and Cr^{III} (spin $s = 3/2$) occupy the 30 sites of an icosidodecahedron, a closed spherical structure consisting of 20 corner-sharing triangles arranged around 12 pentagons. Consequently, this structure serves as a zero-dimensional analogue of the planar Kagome lattice that is composed of corner-sharing triangles arranged around hexagons. Most important, these compounds are realized as crystals of identical molecular units, where intermolecular magnetic interactions are negligible as compared to intramolecular magnetic interactions. Measurements of the magnetic properties therefore reflect those of the common, individual molecular unit.

In previous work it has been shown that the magnetic properties of both molecules can accurately be described by an isotropic nearest-neighbour *classical* Heisenberg model of interacting spins which can be obtained by the following procedure. The *quantum* Hamiltonian operator of the nearest-neighbour Heisenberg single- J model is $J \sum_{(i,j)} \vec{S}_i \cdot \vec{S}_j + g\mu_B \vec{H} \cdot \sum_i \vec{S}_i$. The spin operator \vec{S}_i describes the magnetic ion (spin s) at site i and is given in units of \hbar , the sum includes terms for distinct pairs of nearest-neighbour spins, μ_B is the Bohr magneton, \vec{H} is the external magnetic field. The corresponding classical Heisenberg model is obtained by replacing \vec{S}_i by $\sqrt{s(s+1)}\vec{m}_i$, where \vec{m}_i is a unit vector [11]. The exchange constant of the classical Heisenberg model is thus $J_c = Js(s+1)$. It has been shown [16] for $T = 0$ K that $\langle m_z \rangle_i = H/H_s$ for a magnetic field $\vec{H} = H\vec{e}_z$, for $H < H_s$, and $\langle m_z \rangle_i = 1$ for $H \geq H_s$, and the saturation field is $H_s = 6Js/(g\mu_B)$ [9, 10]. For $T > 5$ K one can use a single antiferromagnetic exchange constant $J_c = Js(s+1)$ (in units of Boltzmann's constant k_B) with values of 13.74 K and 32.63 K for $\{\text{Mo}_{72}\text{Fe}_{30}\}$ and $\{\text{Mo}_{72}\text{Cr}_{30}\}$, respectively [9, 10]. However, recent low temperature and low magnetic field measurements ($T < 5$ K) of the magnetic susceptibility of $\{\text{Mo}_{72}\text{Fe}_{30}\}$ and $\{\text{Mo}_{72}\text{Cr}_{30}\}$ have revealed the existence of a modified interaction scenario where the 60 nearest-neighbour interactions are not identical. Instead, the exchange interactions are disordered, characterized by a two-parameter probability distribution whose mean value is J_c [10].

The layout of this paper is as follows. In section 2 we explore the consequences of exchange disorder using the classical Heisenberg model. In particular we present our simulational results for four quantities, each of which exhibits striking evidence for spin freezing or slow magnetization dynamics. In section 3 we present our experimental results for proton line width in both $\{\text{Mo}_{72}\text{Fe}_{30}\}$ and $\{\text{Mo}_{72}\text{Cr}_{30}\}$ for temperatures below 1 K. The rapid and large increase of the observed line width on cooling is suggestive of spin freezing. Finally, our results are summarized in section 4.

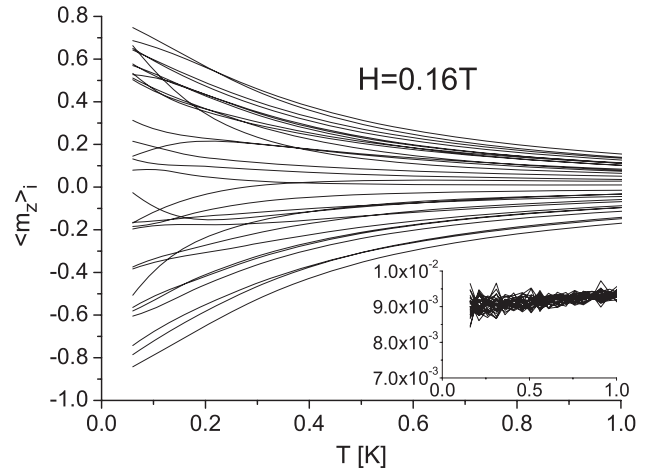


Figure 1. Results of classical Monte Carlo simulations, using a protocol as described in the text, for a model system of $\{\text{Mo}_{72}\text{Fe}_{30}\}$ in a magnetic field $\vec{H} = H\vec{e}_z$, where $H = 0.16$ T. As discussed in the text, due to exchange disorder the local spin variables $\langle m_z \rangle_i$ of the 30 iron sites display spin freezing. In the absence of exchange disorder (inset) the simulation results are independent of i and approach the exact $T = 0$ K theoretical result of [16], $\langle m_z \rangle_i = H/H_s = 9.04 \times 10^{-3}$, independent of i .

2. Simulations

We find manifestations of spin freezing and slow magnetization dynamics, due to the exchange disorder in both molecules, in four distinct calculated quantities: (1) the thermal averaged *local* moments in a single molecule; (2) the time decay of the thermoremanent dc magnetization (TRM); (3) the field cooled (FC) and zero-field cooled (ZFC) susceptibility; and (4) ground state properties. Using the probability distribution parameters as given in [10] the exchange couplings for the 60 nearest-neighbour pairs are chosen to be uniformly distributed in the range $[(1 - \rho)J_c, (1 + \rho)J_c]$, where the half width of the distribution is chosen as $\rho = 0.4$, and the mean of the distribution, J_c , is listed earlier. By comparison, for a single- J scenario (i.e., without exchange disorder) we find that spin freezing and slow magnetization dynamics are absent.

In figure 1 we show the thermal average of the classical spin variable $\langle m_z \rangle_i$ due to a magnetic field $\vec{H} = H\vec{e}_z$ for $H = 0.16$ T as a function of temperature for the 30 iron sites (labelled by the index i) for the exchange disorder model of $\{\text{Mo}_{72}\text{Fe}_{30}\}$ as obtained by classical Monte Carlo simulations. This choice of field was selected to match the value for our NMR measurement described in section 3. The protocol for such a simulation is as follows: we start at the highest temperature value of $T = 1.1$ K and apply an external field of $H = 0.16$ T in the z -direction. Using random initial conditions we perform 2×10^7 Monte Carlo steps for pre-conditioning. After that thermal averages are calculated by sampling the system over 10^9 Monte Carlo steps. This protocol is repeated for all lower temperatures in steps of $\Delta T = 0.05$ K until the lowest temperature is reached.

For temperatures larger than $T \approx 1$ K the $\langle m_z \rangle_i$ are nearly independent of i and proportional to H , and the results are in agreement with those for the single- J model for all T

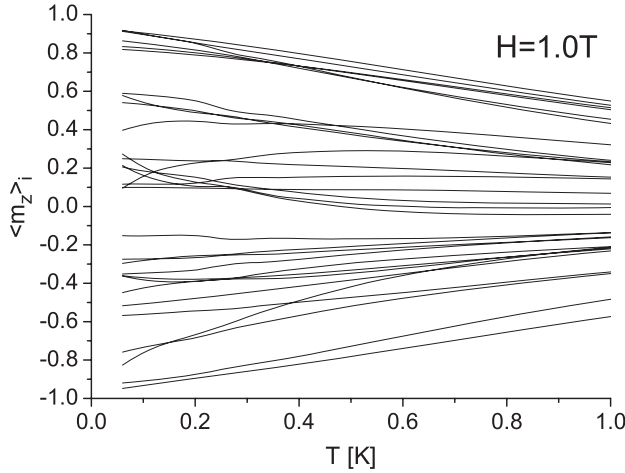


Figure 2. Results of classical Monte Carlo simulations for a model system of $\{\text{Mo}_{72}\text{Cr}_{30}\}$ in a magnetic field $\vec{H} = H\vec{e}_z$, where $H = 1.0\text{ T}$, using a protocol as described in the text. As in the case of $\{\text{Mo}_{72}\text{Fe}_{30}\}$ the local spin variables $\langle m_z \rangle_i$ of the 30 chromium sites display spin freezing due to exchange disorder. Note, because of a much larger average exchange constant and a larger external field the variation of $\langle m_z \rangle_i$ with T is more gradual than for $\{\text{Mo}_{72}\text{Fe}_{30}\}$ shown in figure 1.

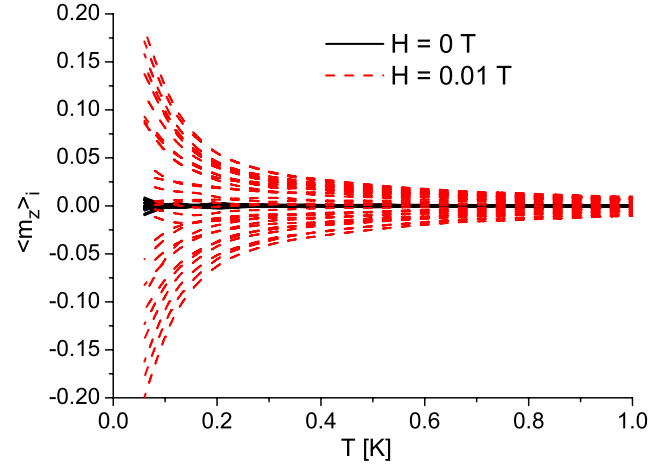


Figure 3. Results of classical Monte Carlo simulations for a model system of $\{\text{Mo}_{72}\text{Fe}_{30}\}$ in zero field (black lines) and in a weak magnetic field of $H = 0.01\text{ T}$ (dashed red lines). As discussed in the text, in the absence of a field component the thermal averages of the local spin variables $\langle m_z \rangle_i$ (as well as $\langle m_x \rangle_i$ and $\langle m_y \rangle_i$) are zero because of the isotropic Hamiltonian. Applying a weak field (0.01 T) in the z -direction breaks this symmetry and the spectrum of robust diverse nonzero averages of the $\langle m_z \rangle_i$ is restored.

(see inset). However, below $T \approx 1\text{ K}$ the set of values of $\langle m_z \rangle_i$ strongly depends on i and collectively spans almost the entire range from -1 to $+1$. Using the simulational protocol as described above we show in figure 2 the same data for the exchange disorder model of $\{\text{Mo}_{72}\text{Cr}_{30}\}$ for an external field of $H = 1.0\text{ T}$, again to match the choice for the NMR measurement described in section 3. Because of a much larger average exchange constant and a larger external field the broadening is more gradual than for $\{\text{Mo}_{72}\text{Fe}_{30}\}$ but the set of values of $\langle m_z \rangle_i$ again strongly depends on i and collectively spans almost the entire range from -1 to $+1$ at the lowest temperature. As in the case of $\{\text{Mo}_{72}\text{Fe}_{30}\}$ we find that in the absence of exchange disorder the simulation results for $\langle m_z \rangle_i$ are independent of i and, for decreasing T , approach the exact $T = 0\text{ K}$ theoretical result of [16].

Thus, in the exchange disordered case in both molecules, there exists a preferred direction parallel or anti-parallel to the direction of the external field that persists during the averaging process, i.e. the spins are *frozen* below 1 K. It is important to note that the local $\langle m_z \rangle_i$ are not snapshots of a particular spin configuration at a specific time but rather the value of the *thermal average* numerically obtained by standard state space sampling during the Monte Carlo simulation. Not shown in the figure are the thermal averages of the local spin variables $\langle m_x \rangle_i$ and $\langle m_y \rangle_i$ which are zero for all temperatures. This result is expected for the present Hamiltonian of a small-sized, spherical magnetic molecule consisting of Heisenberg spins. In the absence of a field component the magnetic system may be able to rotate as a whole (giving zero thermal averages $\langle m_k \rangle_i$ for any of the $k = x, y, z$ components), even below the freezing temperature. Indeed, the calculated averages from our Monte Carlo simulations, shown in figure 3, behave in this manner. It is important, however, to note from figure 3 that even a very weak field (0.01 T) breaks the rotational symmetry

and restores the spectrum of robust diverse nonzero averages of the $\langle m_z \rangle_i$ while the perpendicular components $\langle m_x \rangle_i$ and $\langle m_y \rangle_i$ remain zero, i.e. are not ‘pinned’. We suggest that this body of Monte Carlo data be understood in terms of the following *dynamical* picture (which is entirely absent in the Monte Carlo method): due to the exchange disorder, at low temperatures in zero magnetic field the individual spin vectors move so slowly that they appear to be frozen when observed even over long but finite time intervals, yet the infinite time average of any spin component is zero. Even a weak magnetic field, say in the z -direction, is sufficient to freeze the m_{zi} , and its frozen value is provided by the nonzero Monte Carlo average $\langle m_z \rangle_i$. This motivates the study based on spin dynamics that is summarized below, which reveals slow magnetization dynamics due to the exchange disorder.

Other indications of spin freezing include the slow relaxation of the TRM in the freezing regime and a characteristic difference between FC and ZFC susceptibilities. The simulation of these properties requires a realistic description of the relaxational, non-equilibrium spin dynamics of the system. Since Monte Carlo methods randomly generate spin configurations without any relation to the underlying spin equations of motion one needs other methods, namely heat bath simulational methods that couple the spin equations of motion to a heat bath. An effective method for investigating relaxational properties is to use the numerical solution of the stochastic Landau–Lifshitz equation which simulates the time evolution of the spin system coupled to the heat bath according to a Langevin approach [17]. Fluctuating fields are used to account for the effects of the interaction of the spin system with the heat bath. Those environmental degrees of freedom are also responsible for the damped precession of the magnetization parameterized by a phenomenological damping factor λ . The value of λ is unknown for the systems under study, so we have

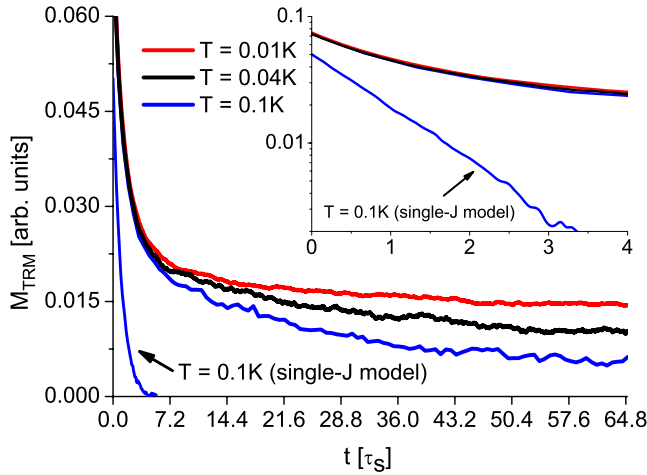


Figure 4. Simulated TRM time decays of the FC magnetization ($H_{FC} = 0.1$ T) of a model system of $\{Mo_{72}Fe_{30}\}$ with and without exchange disorder for temperatures given in the legends. The time variable is scaled in units of the lifetime, τ_s , of the single- J model, as explained in the text. In the inset we show a semi-log plot of the time decays in the short-time regime. In contrast to the exchange disordered model, one clearly sees that the single- J model of $\{Mo_{72}Fe_{30}\}$ (the lowest curve) shows a fast exponential decay, as expected for a magnetic system with a flat free-energy landscape.

chosen $\lambda = 0.1$ which is a common value used in the study of magnetization relaxation in nanoparticles [18].

Figure 4 shows our simulation results for TRM time decays of the FC magnetization ($H_{FC} = 0.1$ T) of a model system of $\{Mo_{72}Fe_{30}\}$ with and without exchange disorder. We have used the following simplified protocol for such a simulation: the system is cooled in a field $H_{FC} = 0.1$ T to a measuring temperature T_m in the freezing regime. This is done at a rate of 10^7 time steps K^{-1} . At T_m the field is suddenly reduced to zero. The subsequent relaxation of the magnetization is then sampled. To achieve satisfactory statistics we have performed averages over 100 identical model systems. We have performed simulations at $T_m = 0.1$ K for both the exchange disordered and the single- J model for a direct comparison. In the inset of figure 4 we show a semi-log plot of the time decays in the short-time regime. One clearly sees that the single- J model of $\{Mo_{72}Fe_{30}\}$ (the lowest curve) shows a fast exponential decay as expected for a magnetic system with a flat free-energy landscape. For further comparison we have determined the corresponding lifetime τ_s , and use that as our time unit. The upper three curves correspond to the exchange disordered model for $T_m = 0.1, 0.04$, and 0.01 K. Here, we find non-exponential decay with identical characteristics independent of temperature. In the main panel of figure 4 we show the long-time behaviour of the TRM decay. For the exchange disordered model the rapid relaxation within the first $5\tau_s$ is followed by a very slow decay. A first analysis of the functional form of the time decay is approximately consistent with a $\log(t)$ dependence for $t > 8\tau_s$. However, further detailed simulations are needed to establish an accurate functional form.

In figure 5 we show our results for the FC and ZFC susceptibility for a model of $\{Mo_{72}Fe_{30}\}$ with and without

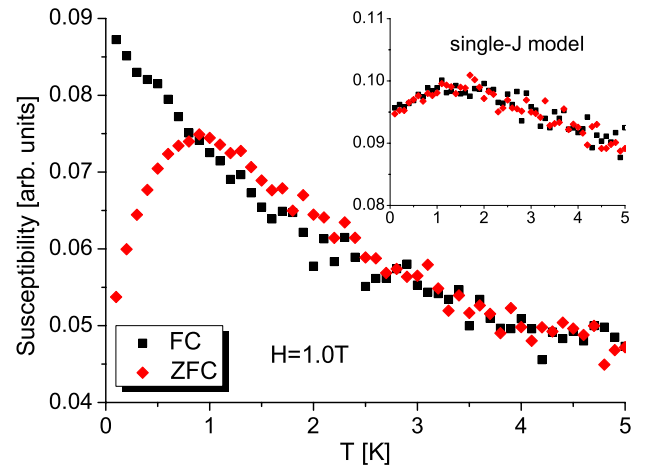


Figure 5. Simulation of FC and ZFC susceptibility for a model system of $\{Mo_{72}Fe_{30}\}$ with and without (inset) exchange disorder. The FC curve was obtained by using an external field of $H = 1.0$ T; the parameters of the simulation procedure are given in the text.

(inset) exchange disorder again by solving numerically the stochastic Landau–Lifshitz equation. In our simulations the system is cooled down from $T = 5.0$ K in zero field at a rate of 2×10^7 time steps per K^{-1} . At $T = 0.1$ K an external field of $H = 1.0$ T is switched on and the system is heated up to $T = 5.0$ K at the same rate while the magnetization is sampled. The system is again cooled down yielding the FC curve. The behaviour shown in figure 5 is consistent with that for spin glass systems, namely a characteristic difference between the FC and ZFC curves below a certain branching temperature which is $T \approx 1$ K in our case. We also find that the branching of the FC and ZFC curves is field dependent: with increasing field the branching temperature is reduced. As shown in the inset, for the single- J case there is no significant difference between the FC and ZFC susceptibilities.

Our fourth piece of evidence for spin freezing and slow magnetization dynamics in model systems of $\{Mo_{72}Fe_{30}\}$ and $\{Mo_{72}Cr_{30}\}$ is based on the calculation of classical ground state properties. For spin glasses one expects a highly degenerate free-energy landscape with a distribution of barriers between different metastable states. Using spin dynamics with Landau–Lifshitz damping we have performed 1000 simulations at $T = 0$ and $H = 0$ starting from different random initial spin configurations and subsequent relaxation. The damping term generally drives the spin configuration towards a minimum of the total energy. We have performed such simulations for a single- J scenario as well as for an exchange disordered one. In the first case there exists a unique classical ground state with a minimal energy value as given in [16]. However, in the disordered case we find a distribution of spin configurations of low energies, but cannot identify a unique ground state. These configurations have energies that are equivalent within a few per cent of each other, supporting the picture that in the exchange disordered case the free-energy landscape consists of a distribution of barriers between different metastable states.

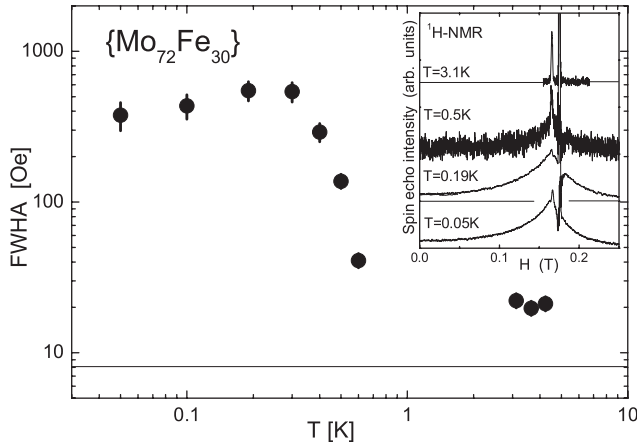


Figure 6. Proton NMR line width in $\{\text{Mo}_{72}\text{Fe}_{30}\}$ for $H = 0.16$ T. The horizontal line gives the T independent nuclear dipolar width. The inset shows some proton NMR spectra measured at $f = 7.03$ MHz at different temperatures (the narrow shifted line is the ^{19}F NMR marker).

3. NMR proton line width

We have performed proton NMR measurements on both $\{\text{Mo}_{72}\text{Fe}_{30}\}$ and $\{\text{Mo}_{72}\text{Cr}_{30}\}$. The polycrystalline samples of $\{\text{Mo}_{72}\text{Fe}_{30}\}$ and $\{\text{Mo}_{72}\text{Cr}_{30}\}$ were synthesized as reported in [7] and [8], respectively. A part of the sample was from the same batch used in a previous magnetization study [10]. NMR provides a local probe sensitive to the local spin components of the magnetic moments via the nuclear–electron dipolar interaction. The second moment of the proton NMR line due to the interaction with the Fe (Cr) moments in the paramagnetic state is given by $\langle \Delta v^2 \rangle = \sum_i \langle (v_R^i - v_0)^2 \rangle = \sum_i \gamma^2 [\sum_j \langle m_z \rangle_j A(\theta_{ij}) / r_{ij}^3]^2$ where $A(\theta_{ij}) / r_{ij}^3$ are the dipolar coupling constants between nucleus i and electron moment j , v_R^i is the resonance frequency of nucleus i and v_0 is the Larmor frequency of the proton with gyromagnetic ratio γ . However, in the spin freezing regime the local spin moments fluctuate with a very low frequency. This frequency is smaller than the NMR frequency and gives rise to a dramatic increase of the proton line width which would be saturated at low enough temperature. Such broadening would be absent for the single- J scenario where the local magnetic moment is the same at each lattice site, proportional to the external field, and spin freezing does not occur.

In figure 6 we show the proton line width data for $\{\text{Mo}_{72}\text{Fe}_{30}\}$ at a low external magnetic field of 0.16 T. A dramatic broadening of the line width is clearly observed starting at about 600 mK. The corresponding proton NMR spectra for several temperatures are shown in the inset of the figure. As can be seen in the spectra at 0.19 and 0.05 K of the inset of figure 6, a residual proton NMR signal can be observed even at $H = 0$ T. Since the internal field at proton sites is generated by Fe spin moments, this is direct evidence of very slow fluctuations of the Fe spin moments even in zero external magnetic field. It is important to point out that the dramatic broadening of the line width in $\{\text{Mo}_{72}\text{Fe}_{30}\}$ below 600 mK does not originate from three-dimensional magnetic ordering

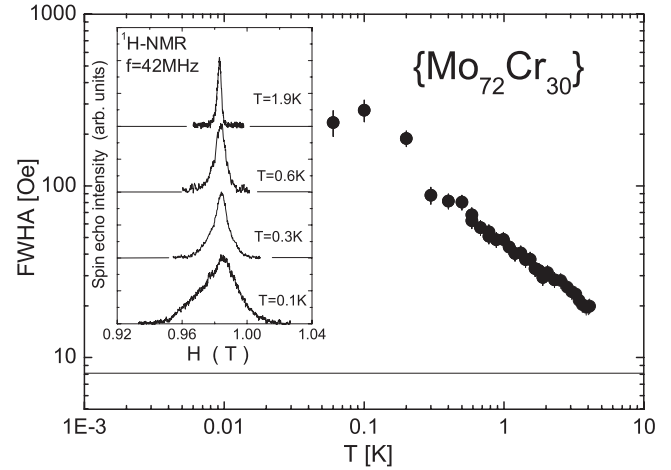


Figure 7. Proton NMR line width in $\{\text{Mo}_{72}\text{Cr}_{30}\}$ for $H = 1$ T. The horizontal line gives the T independent nuclear dipolar widths. The inset shows some proton NMR spectra measured at $f = 42$ MHz at different temperatures.

because magnetic susceptibility measurements on this system, specifically of dM/dH versus H for T down to as low as 60 mK, have been quantitatively reproduced by the exchange disorder model (see figure 4 of [10]).

Low temperature NMR line broadening and zero-field NMR spectra were previously observed in magnetic molecules with a magnetic ground state such as $\{\text{Mn}_{12}\}$ [12] and $\{\text{Fe}_8\}$ [13], but not observed in molecules with a spin singlet ground state [14, 15]. A ferrimagnetic frozen superparamagnetic state like in $\{\text{Mn}_{12}\}$ and $\{\text{Fe}_8\}$ can be ruled out because of the lack of a large anisotropy energy barrier for spin reorientation. On the other hand, the spin freezing due to exchange disorder discussed theoretically above offers a plausible explanation for the observation of a low temperature NMR broadening and zero-field NMR signals in $\{\text{Mo}_{72}\text{Fe}_{30}\}$. The presence of many excited states very close to the ground state, caused by the disorder in the exchange interactions, can lead to the observation by NMR of a local static moment at finite temperature. This does not occur in the antiferromagnetic ring compounds discussed in [14, 15], where, due to the absence of exchange disorder, there are large energy gaps from the singlet ground state to the excited states.

In order to relate the observed broadening to our simulational results shown in figure 1, we have to emphasize that a frozen state in NMR is defined by the spin *dynamics*, i.e. the state in which the correlation time of the fluctuations of the local moments $\langle m_z \rangle_i$ become of the order of the static nuclear–electron dipolar interaction. The corresponding temperature determines the *onset* of the broadening while the proton line width itself is determined by the *static* thermal distribution of the local moments $\langle m_z \rangle_i$. Since the Monte Carlo simulations can only determine the static thermal averages of the local moments $\langle m_z \rangle_i$ we do not expect any abrupt changes to be visible in figure 1.

We observed a similar significant broadening of line width in $\{\text{Mo}_{72}\text{Cr}_{30}\}$ at low temperatures, as shown in figure 7. The inset shows proton NMR spectra for several temperatures.

It will be noted that the broadening in $\{\text{Mo}_{72}\text{Cr}_{30}\}$ is more gradual than for $\{\text{Mo}_{72}\text{Fe}_{30}\}$. This is due to both the higher external field and the larger average exchange interaction in the case of $\{\text{Mo}_{72}\text{Cr}_{30}\}$. As shown in figures 1 and 2, these two effects produce larger local moments $\langle m_z \rangle_i$ for $\{\text{Mo}_{72}\text{Cr}_{30}\}$ than that for $\{\text{Mo}_{72}\text{Fe}_{30}\}$. The larger $\langle m_z \rangle_i$ are responsible for a broader line width even above the spin freezing temperature, thus a sudden increase of the line width would be smeared out in the case of $\{\text{Mo}_{72}\text{Cr}_{30}\}$ just below the spin freezing temperature. Although a specific spin freezing temperature defined by NMR measurement cannot be determined for $\{\text{Mo}_{72}\text{Cr}_{30}\}$, the broadening of the line width at very low temperatures down to 60 mK is consistent with a spin freezing state. The solid horizontal line in each graph, marking the value of the T independent nuclear dipolar width, gives an idea of what the width would be without the contribution of local moments at the Fe (Cr) sites.

We have estimated the static nuclear–electron dipolar interaction for $\{\text{Mo}_{72}\text{Fe}_{30}\}$ to be of the order of 500 Oe (or 2 MHz) from the limiting low temperature line width in figure 6. In $\{\text{Mo}_{72}\text{Cr}_{30}\}$ the limiting line width is smaller than that of $\{\text{Mo}_{72}\text{Fe}_{30}\}$ in spite of the higher applied magnetic field, reflecting the fact that the susceptibility, and thus also the static nuclear–electron dipolar field, is smaller by more than a factor of two [10]. We conclude from the low temperature broad spectra which extends down to zero external field that the fluctuation frequency of Fe spin moments at low temperature becomes slower than the megahertz range. Thus in both molecules $\{\text{Mo}_{72}\text{Fe}_{30}\}$ and $\{\text{Mo}_{72}\text{Cr}_{30}\}$ the NMR results are consistent with the above-discussed theoretical scenario of spin freezing due to exchange disorder. It should, however, be pointed out that the NMR results at low temperature would also be consistent with any configuration of frozen, static, local Fe magnetic moments.

4. Summary

The major finding of this paper is that, due to disorder of the intramolecular exchange interactions, the pair of geometrically frustrated magnetic molecules $\{\text{Mo}_{72}\text{Fe}_{30}\}$ and $\{\text{Mo}_{72}\text{Cr}_{30}\}$ is expected, for temperatures below 1 K, to display characteristics of spin freezing and slow dynamics reminiscent of spin glass behaviour. As spelt out in section 2, these characteristics are manifested in four distinct quantities that we have explored by applying simulational methods to a classical Heisenberg model of these magnetic molecules. In particular, due to exchange disorder, in weak magnetic fields the calculated thermal equilibrium value of the individual spin moment vector is broadly distributed across the 30 spins of the individual magnetic molecules for temperatures below 1 K, behaviour that we refer to as spin freezing. As explained in section 3, an expected experimental signature of spin freezing is a steep increase of the proton NMR line width on cooling. Indeed, we have observed strong line width broadening (see figures 6 and 7) upon cooling samples of both $\{\text{Mo}_{72}\text{Fe}_{30}\}$ and $\{\text{Mo}_{72}\text{Cr}_{30}\}$ below 1 K.

As shown by our simulations, exchange disorder leads to a free-energy landscape for the spin configurations in the individual magnetic molecule that consists of a distribution of barriers between different metastable states. As a result of this we find a slow time decay of the thermoremanent dc magnetization and a characteristic difference between FC and ZFC susceptibilities in both molecules $\{\text{Mo}_{72}\text{Fe}_{30}\}$ and $\{\text{Mo}_{72}\text{Cr}_{30}\}$ for temperatures below 1 K.

We hope that these features will be put to direct experimental tests in the near future. This would provide the opportunity to study glassy spin dynamics in *zero-dimensional* systems not just theoretically, but also experimentally, and to compare them with the behaviour of bulk spin glass systems.

Acknowledgments

We acknowledge the contribution of D Procissi and A Lascialfari. Research performed by CS is supported by the DFG Research Group 945. The work was in part supported by Grant-in-Aid on Priority Area ‘Novel States of Matter Induced by Frustrations’ from the Ministry of Education, Culture, Sports, Science and Technology of Japan. Work at the Ames Laboratory was supported by the Department of Energy-Basic Energy Sciences under contract No. DE-AC02-07CH11358.

References

- [1] Greedan J 2001 *J. Mater. Chem.* **11** 37
- [2] Ramirez A P 1994 *Annu. Rev. Mater. Sci.* **24** 453
Schiffer P and Ramirez A P 1996 *Comments Condens. Matter Phys.* **18** 21
- [3] Saunders T E and Chalker J T 2007 *Phys. Rev. Lett.* **98** 157201
- [4] Chalker J T, Holdsworth P C W and Shender E F 1992 *Phys. Rev. Lett.* **68** 855
- [5] Lee J D 2005 *J. Magn. Magn. Mater.* **292** 462
- [6] Binder K and Young A P 1986 *Rev. Mod. Phys.* **58** 801
- [7] Müller A, Sarkar S, Shah S Q N, Bögge H, Schmidtman M, Sarkar S, Kögerler P, Hauptfleisch B, Trautwein A and Schünemann V 1999 *Angew. Chem. Int. Edn Engl.* **38** 3238
- [8] Todea A M, Merca A, Bögge H, van Slageren J, Dressel M, Engelhardt L, Luban M, Glaser T, Henry M and Müller A 2007 *Angew. Chem. Int. Edn* **46** 6106
- [9] Müller A, Luban M, Schröder C, Modler R, Kögerler P, Axenovich M, Schnack J, Canfield P C, Bud'ko S and Harrison N 2001 *ChemPhysChem* **2** 517
- [10] Schröder C, Prozorov R, Kögerler P, Vannette M D, Fang X, Luban M, Matsuo A, Kindo K, Müller A and Todea A M 2008 *Phys. Rev. B* **77** 224409
- [11] Ciftja O, Luban M, Auslender M and Luscombe J H 1999 *Phys. Rev. B* **60** 10122
- [12] Furukawa Y, Watanabe K, Kumagai K, Jang Z H, Lascialfari A, Borsa F and Gatteschi D 2000 *Phys. Rev. B* **62** 14246
- [13] Furukawa Y, Kumagai K, Lascialfari A, Aldrovandi S, Borsa F, Sessoli R and Gatteschi D 2001 *Phys. Rev. B* **64** 094439
- [14] Lascialfari A, Gatteschi D, Borsa F and Cornia A 1997 *Phys. Rev. B* **55** 14341
- [15] Maegawa S and Sasaki Y 2006 *J. Phys. Soc. Japan* **75** 034710
- [16] Axenovich M and Luban M 2001 *Phys. Rev. B* **63** 100407(R)
- [17] Antropov V P, Tretyakov S V and Harmon B N 1997 *J. Appl. Phys.* **81** 3961
- [18] García-Palacios J L and Lázaro F J 1998 *Phys. Rev. B* **58** 14937